

A novel ethanol/oxygen microfluidic fuel cell with enzymes immobilized onto cantilevered porous electrodes

D Desmaële^{1,2}, T T Nguyen-Boisse¹, L Renaud³ and S Tingry¹

¹Institut Européen des Membranes, UMR 5635, ENSCM-UMI-CNRS, place Eugène Bataillon, 34095 Montpellier, France

²Now at Istituto Italiano di Tecnologia (IIT), Center for Biomolecular Nanotechnologies, Via Barsanti, 73010, Arnesano, (Lecce), Italy

³Université de Lyon, Institut des Nanotechnologies de Lyon INL-UMR5270, CNRS, Université Lyon 1, Villeurbanne F-69622, France

E-mail: denis.desmaele@iit.it

Abstract. This paper introduces a novel design of membraneless microfluidic biofuel cell that incorporates three-dimensional porous electrodes containing immobilized enzymes to catalyze redox reactions occurring in the presence of ethanol/O₂ co-laminar flows. In order to maximize the penetration depth of the reactants inside the porous medium, we report on the preliminary evaluation of cantilevered bioelectrodes, namely the fibrous electrodes protrude along the internal walls of the miniature electrochemical chamber. As a first proof-of-concept, we demonstrate the integration of a bioanode and a biocathode into a lamination-based microfluidic cell fabricated via rapid prototyping. With enzymes deposited into the fibrous structure of 25 mm long, 1 mm wide and 0.11 mm thick carbon paper electrodes, the volumetric power density reached 1.25 mW cm⁻³ at 0.43 V under a flow rate of 50 μ L min⁻¹. An advantage of the presented microfluidic biofuel cell is that it can be adapted to include a larger active electrode volume via the vertical stacking of multiple thin bioelectrodes. We therefore envision that our design would be amenable to reach the level of net power required to supply energy to a plurality of low-consumption electronic devices.

1. Introduction

Co-laminar enzymatic biofuel cells (CL-EFCs) are envisioned as a promising option for supplying power to low-consumption electronic devices [1]. It is indeed recognized that CL-EFCs can offer distinctive features: i) unlike conventional fuel cells, a proton exchange membrane is not required; ii) precious metal catalysts can be replaced by low-cost biocatalysts; iii) a variety of readily available fuels can be employed; iv) membraneless CL-EFCs are inherently well adapted to miniaturization. Despite such potential advantages, the practical deployment of CL-EFCs is still hindered by limited power yields. To alleviate this hindrance, three-dimensional porous electrodes (3D-PEs) show great potential. Indeed, 3D-PEs offer enlarged reactive surfaces compared to conventional two-dimensional electrodes. Notable performance improvements were therefore reported for co-laminar fuel cells exploiting 3D-PEs with chemical reactants [2]. Similarly, 3D-PEs would allow for higher enzyme loadings in CL-EFCs. To the best of the authors' knowledge, however, most designs of CL-EFCs that can be found in the literature still



rely on soluble enzyme catalysts flowing over gold electrodes or on enzymes immobilized onto modified flat surfaces [3, 4]. Here, we introduce and evaluate a novel lamination-based CL-EFC that integrates cantilevered 3D-PEs with the aim to reach higher enzyme loadings and improved performance.

2. Experiments

Unless otherwise stated, all chemicals were obtained from Sigma-Aldrich and used as received.

2.1. Preparation of porous bioelectrodes

Toray carbon paper (TCP) was used as the electrode material. TCP sheets purchased were 110 μm thick (TGP-H-030, Toray). They were not coated for wet proofing. Electrode patterns were cut by xurography (i.e., razor writing) using a cutting plotter (CE 6000-40, Graphtec) [5]. Electrode areas which were not intended to be in contact with the reactants were coated with wax. The remaining hydrophilic zones devoted to the subsequent deposition of the enzymes (see dashed lines in figure 1B) were 25 mm long and 1 mm wide (i.e., the area and volume of the bioelectrodes were 0.25 cm^2 and $\approx 0.0028 \text{ cm}^3$, respectively).

For the bioanode, the enzyme alcohol dehydrogenase (ADH) and its cofactor β -nicotinamide adenine dinucleotide sodium salt (NAD^+) were employed for ethanol oxidation. Prior to enzyme immobilization, a first electropolymerized poly(methylene green) film was used as an electrocatalyst. A phosphate buffer solution containing the enzymes was subsequently pipetted onto the poly(methylene green) film and dried at room temperature by performing cyclic voltammetry under nitrogen atmosphere from -0.6 to 1.2 V/SCE (20 cycles, scan rate 50 mV s^{-1}) in a solution of methylene green 0.4 mM in 0.1 M borate buffer pH 9. The methylene green was used as electrocatalyst for NADH oxidation [6]. Then, a solution of 10 mg of ADH (150 U mg^{-1}), 67 μL of carbon nanoparticles powder (15 mg mL^{-1} , Super P, TIMCAL), 5.5 mg NAD^+ , 5 μL polyethylenimine (5% wt), and 25 μL of 0.1 M phosphate buffer pH 7 was mixed in a vortex mixer and 5 μL of the final mixture was pipetted onto the poly(methylene green) film and dried at room temperature.

For the biocathode, *Trametes versicolor* laccase (13.6 U mg^{-1}) was entrapped along with 2,2-azinobis(3-ethylbenzothiazoline-6-sulfonate) diammonium salt (ABTS) in a polypyrrole film for O_2 electroreduction. First, 5 μL of a mixture containing 7.5 mg laccase, 100 μL of carbon nanoparticles powder (15 mg mL^{-1} , Super P, TIMCAL) in 0.1 M phosphate buffer pH 5 was drop-casted on the TCP. After drying at room temperature, pyrrole electropolymerization was performed at +0.6 V/SCE, by dipping the electrode in a solution containing pyrrole (200 mM), ABTS (20 mM) in 0.1 M $\text{NaClO}_4 \text{ H}_2\text{O}$, until a charge of 0.5 C passed. The complete polymerization of any excess pyrrole that may have remained was achieved by cycling the electrode in phosphate buffer (pH 5) from 0 to 0.8 V (5 cycles, scan rate of 50 mV s^{-1}).

2.2. Fabrication of the CL-EFC

Both bioelectrodes were integrated in a T-shaped laminated CL-EFC composed of double-sided pressure adhesive (DSPA) films sandwiched between a glass slide and a Polyethylene naphthalate (PEN) capping layer. The DSPA layers (labeled $T_{j=1,3}$ in figure 1A) were 100 μm thick (Montex-DX 1, X-Film) whereas the PEN layer was 75 μm thick (ES361075, Goodfellow). DSPA and PEN layers were also prepared by xurography using a cutting plotter. For the assembly of the entire structure, we used a CNC-machined mechanical guide (alignment accuracy $\pm 100 \mu\text{m}$). The bioelectrodes were placed in specific grooves patterned in T_2 . The bioelectrodes were thereby centered in the middle of the microchannel (see cross section b-b' in figure 1). We intentionally favored such cantilevered (i.e., protruding) electrodes rather than electrodes conventionally placed at the bottom of the microchannel. Indeed, when fluids flow over bottom, reactants may solely interact with the top portion of the 3D-PEs [2]. For the delivery and removal of

fluids, polytetrafluoroethylene tubing was firmly inserted into the holes of three access ports made of Plexiglas.

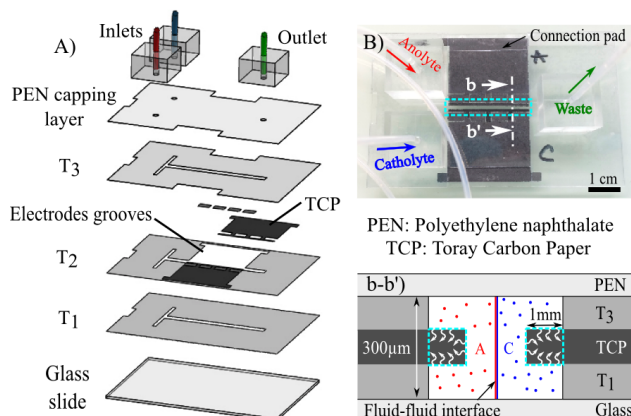


Figure 1. A) Expanded view detailing the design of the CL-EFC. B) Overview of the final CL-EFC after assembly. b-b') Cross-sectional view illustrating the central position of the cantilevered bioelectrodes.

After assembly, tests of the complete CL-EFC containing both bioelectrodes were performed at room temperature. The catholyte solution consisted of phosphate buffer solution (0.1 M, pH 3) saturated with O_2 (2-4 mM [7]). The anolyte solution contained ethanol (40 mM) and NAD^+ (5 mM) in phosphate buffer (0.1 M, pH 9). Solutions were then injected into the CL-EFC using a syringe pump (KDS200, KD Scientific). During experiments, the flow rate was set to $50 \mu L \min^{-1}$ with the aim to avoid potential enzyme leaching. Steady-state polarization data were obtained under potentiostatic control (Autolab, Eco chemie).

3. Results

First, the enzymes immobilized onto the 3D-PEs were visually inspected via scanning electron microscopy (SEM). As can be viewed from figure 2A, the overall surface of the TCP is well covered by the enzyme layer. When observing the thickness of an enzyme-modified TCP, however, it appears that the enzymes do not fully penetrate into the fibrous electrode structure (see comparison to bare TCP in figure 2B). This suggests that our current immobilization protocols should be improved prior to be used with thicker TCP electrodes. Nonetheless, our CL-EFC could be adapted to increase the amount of enzymes exposed to the reactants by stacking multiple thin bioelectrodes such as the ones used here.

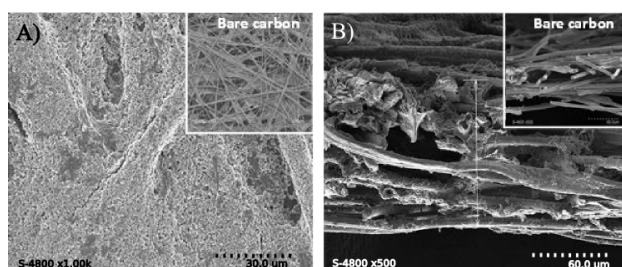


Figure 2. SEM micrographs of a 3D TCP porous bioanode before/after enzyme immobilization. A) Top view. B) Cross sectional view.

The performance of the complete CL-EFC was then evaluated. Figures 3A and 3B show the polarization curve and the power curve obtained, respectively. With no current flowing through an external load, the open circuit voltage is about 0.63 V, which is comparable with values reported elsewhere [8]. When considering the current and power densities normalized to the electrode projected surface area (PSA), our CL-EFC produces a maximum power density of $\approx 14 \mu W \text{ cm}^{-2}$. Although moderate, this power density still compares favorably with some previous works. In [9], a microchip-based bioanode paired with an external Pt cathode working

from ethanol produced $5 \mu\text{W cm}^{-2}$ at 0.34 V. More recently, another ethanol/O₂ CL-EFC delivered $10 \mu\text{W cm}^{-2}$ when using gold bioelectrodes having a length-to-width aspect ratio (AR) of 20 (AR=25 in this work) [10]. A straightforward comparison between different configurations, however, remains delicate. Further, for 3D-PEs, the electrode PSA may be untrue [11]. As discussed elsewhere (e.g., see [2]), we believe that normalization based on the electrode volume provides a more accurate representation of our CL-EFC. In this case, the maximum volumetric power generated by our CL-EFC reaches $\approx 1250 \mu\text{W cm}^{-3}$ at 0.43 V. The corresponding volumetric current density is almost 3 mA cm^{-3} . We believe these volumetric values make more sense for our design, especially if considering that our CL-EFC could be scaled up with multiple stacked thin bioelectrodes offering higher enzyme loading capabilities.

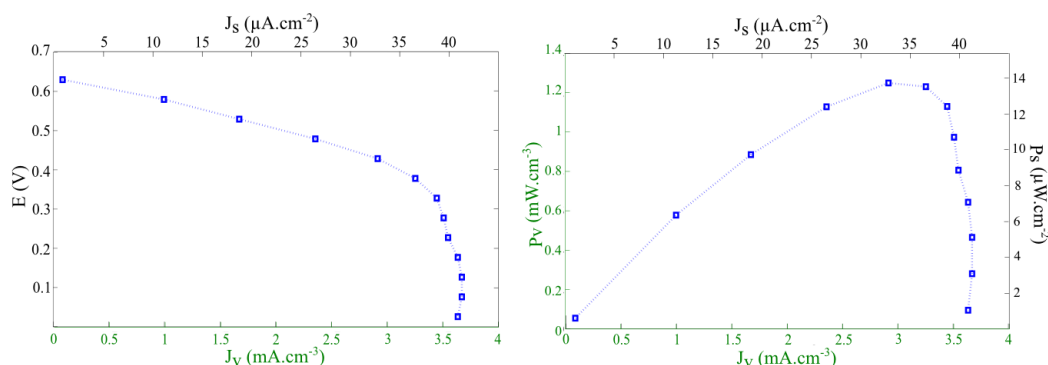


Figure 3. Performance measured for the ethanol/O₂ CL-EFC at $50 \mu\text{L min}^{-1}$: (A) Polarization curve and (B) Power curve.

4. Conclusions

The possibility to reach a volumetric power density of $\approx 1.25 \text{ mW cm}^{-3}$ at 0.43 V with the ethanol/O₂ CL-EFC presented here is encouraging. Indeed, even if considering the power density normalized by the projected surface area ($\approx 14 \mu\text{W cm}^{-2}$), the level of performance achieved can already be sufficient to drive a low-consumption electronic system, as demonstrated in [12]. In the near future, our efforts will be focused on the improvement of our immobilization protocols so that enzymes could be more efficiently attached to thicker carrier matrices. Additionally, we will try to scale up our design by stacking several bioelectrodes to increase the enzyme loading and the net power produced.

References

- [1] Gellett W, Kesmez M, Schumacher J, Akers N and Minter S D 2010 *Electroanalysis* **22** 727–31
- [2] Kjeang E, Michel R, Harrington D A, Djilali N and Sinton D 2008 *J. Am. Chem. Soc.* **130** 4000–6
- [3] Renaud L, Selloum D and Tingry S 2015 *Microfluidics and Nanofluidics* 1–10
- [4] Beneyton T, Wijaya I P M, Salem C B, Griffiths A and Taly V 2013 *Chem. Commun.* **49** 1094–6
- [5] Bartholomeusz D A, Boutté R W and Andrade J D 2005 *Microelectromechanical Systems, Journal of* **14** 1364–74
- [6] Akers N L, Moore C M and Minter S D 2005 *Electrochim. Acta* **50** 2521–5
- [7] Jayashree R S, Gancs L, Choban E R, Primak A, Natarajan D, Markoski L J and Kenis P J 2005 *J. Am. Chem. Soc.* **127** 16758–9
- [8] Neto S A, Forti J, Zucolotto V, Ciancaglini P and De Andrade A 2011 *Biosens. Bioelectron.* **26** 2922–6
- [9] Moore C M, Minter S D and Martin R S 2005 *Lab Chip* **5** 218–25
- [10] Selloum D, Tingry S, Techer V, Renaud L, Innocent C and Zouaoui A 2014 *J. Power Sources* **269** 834–40
- [11] Sharma M, Bajracharya S, Gildemyn S, Patil S A, Alvarez-Gallego Y, Pant D, Rabaey K and Dominguez-Benetton X 2014 *Electrochim. Acta* **140** 191–208
- [12] Desmaële D, Renaud L and Tingry S 2015 *Sens. Actuators B* **220** 583–9